

1 **Identification of 19 new risk loci and potential regulatory mechanisms influencing susceptibility to**  
2 **testicular germ cell tumour**

3 Kevin Litchfield<sup>1</sup>, Max Levy<sup>1</sup>, Giulia Orlando<sup>1</sup>, Chey Loveday<sup>1</sup>, Philip J. Law<sup>1</sup>, Gabriele Migliorini<sup>1</sup>, Amy  
4 Holroyd<sup>1</sup>, Peter Broderick<sup>1</sup>, Robert Karlsson<sup>2</sup>, Trine B Haugen<sup>3</sup>, Wenche Kristiansen<sup>3</sup>, Jérémie  
5 Nsengimana<sup>4</sup>, Kerry Fenwick<sup>5</sup>, Ioannis Assiotis<sup>5</sup>, ZSofia Kote-Jarai<sup>1</sup>, Alison M. Dunning<sup>6</sup>, Kenneth  
6 Muir<sup>8,9</sup>, Julian Peto<sup>10</sup>, Rosalind Eeles<sup>1,11</sup>, Douglas F Easton<sup>6,7</sup>, Darshna Dudakia<sup>1</sup>, Nick Orr<sup>12</sup>, Nora  
7 Pashayan<sup>13</sup>, UK Testicular Cancer Collaboration\*, The PRACTICAL consortium\*, D. Timothy Bishop<sup>4</sup>,  
8 Alison Reid<sup>14</sup>, Robert A Huddart<sup>15</sup>, Janet Shipley<sup>16</sup>, Tom Grotmol<sup>17</sup>, Fredrik Wiklund<sup>2</sup>, Richard S  
9 Houlston<sup>1</sup>, Clare Turnbull<sup>1,18, 19</sup>

- 10 1. Division of Genetics & Epidemiology, The Institute of Cancer Research, London, SM2 5NG, UK  
11 2. Department of Medical Epidemiology and Biostatistics, Karolinska Institutet, Stockholm, 171  
12 77, Sweden  
13 3. Faculty of Health Sciences, Oslo and Akershus University College of Applied Sciences, Oslo,  
14 Norway  
15 4. Section of Epidemiology & Biostatistics, Leeds Institute of Cancer and Pathology, Leeds, LS9  
16 7TF, UK  
17 5. Tumour Profiling Unit, The Institute of Cancer Research, London, SW3 6JB, UK  
18 6. Centre for Cancer Genetic Epidemiology, Department of Oncology, University of Cambridge,  
19 Cambridge, CB1 8RN, UK  
20 7. Centre for Cancer Genetic Epidemiology, Department of Public Health and Primary Care,  
21 University of Cambridge, Cambridge, CB1 8RN, UK  
22 8. Division of Health Sciences, Warwick Medical School, Warwick University, CV4 7AL, UK  
23 9. Institute of Population Health, University of Manchester, M1 3BB, UK  
24 10. Department of Non-Communicable Disease Epidemiology, London School of Hygiene and  
25 Tropical Medicine, London, United Kingdom.

- 26 11. Royal Marsden NHS Foundation Trust, London, SM2 5NG, UK
- 27 12. The Breast Cancer Now Toby Robins Research Centre, The Institute of Cancer Research, 237  
28 Fulham Road, London SW3 6JB, UK
- 29 13. Department of Applied Health Research, University College London, London, WC1E 6BT, UK
- 30 14. Academic Uro-oncology Unit, The Royal Marsden NHS Foundation Trust, Sutton, Surrey, SM2  
31 5PT, UK
- 32 15. Academic Radiotherapy Unit, Institute of Cancer Research, Sutton, Surrey, SM2 5NG, UK
- 33 16. Division of Molecular Pathology, The Institute of Cancer Research, London, SM2 5NG, UK
- 34 17. Cancer Registry of Norway, Oslo, Norway.
- 35 18. William Harvey Research Institute, Queen Mary University, London, EC1M 6BQ, UK
- 36 19. Guys and St Thomas Foundation NHS Trust, Great Maze Pond, London, SE1 9RT, UK

37 \* See supplementary note

38 Correspondence to: Clare Turnbull, Division of Genetics and Epidemiology, The Institute of Cancer  
39 Research, London, SM2 5NG, UK; Tel: ++44 (0) 208 722 4485; E-mail: [clare.turnbull@icr.ac.uk](mailto:clare.turnbull@icr.ac.uk)

40

41 **Key words:** Testicular Cancer, Germ Cell Tumour, TGCT, GWAS, Oncoarray.

42

43 **Genome-wide association studies (GWAS) have transformed our understanding of testicular germ**  
44 **cell tumour (TGCT) susceptibility but much of the heritability remains unexplained. Here we report**  
45 **a new GWAS, a meta-analysis with previous GWAS and a replication series, totalling 7,319 TGCT**  
46 **cases and 23,082 controls. We identify 19 new TGCT risk loci, approximately doubling the number**  
47 **of known TGCT risk loci to 44. By performing *in-situ* Hi-C in TGCT cells, we provide evidence for a**  
48 **network of physical interactions between all 44 TGCT risk SNPs and candidate causal genes. Our**  
49 **findings reveal widespread disruption of developmental transcriptional regulators as a basis of**  
50 **TGCT susceptibility, consistent with failed primordial germ cell differentiation as an initiating step**  
51 **in oncogenesis<sup>1</sup>. Defective microtubule assembly and dysregulation of KIT-MAPK signalling also**  
52 **feature as recurrently disrupted pathways. Our findings support a polygenic model of risk and**  
53 **provide insight into the biological basis of TGCT.**

54

55

56

57

58

59

60

61 Testicular germ cell tumour (TGCT) is the most common cancer in men aged 18-45, with over 52,000  
62 new cases diagnosed annually worldwide<sup>2</sup>. The development of TGCT is strongly influenced by  
63 inherited genetic factors, which contributes to nearly half of all disease risk<sup>3</sup> and is reflected in the 4-  
64 to-8 fold increased risk shown in siblings of cases<sup>4-7</sup>. Our understanding of TGCT susceptibility has  
65 been transformed by recent genome-wide association studies (GWAS), which have so far identified  
66 25 independent risk loci for TGCT<sup>8-18</sup>. Although projections indicate that additional risk variants for  
67 TGCT can be discovered by GWAS<sup>19</sup>, studies to date have been based on comparatively small sample  
68 sizes which have had limited power to detect common risk variants<sup>20</sup>.

69 To gain a more comprehensive insight into TGCT aetiology we performed a new GWAS with  
70 substantially increased power, followed by a meta-analysis with existing GWAS and replication  
71 genotyping (totalling 7,319 cases/23,082 controls). Here we report both the discovery of 19 new  
72 TGCT susceptibility loci and refined risk estimates for the previously reported loci. In addition, we  
73 have investigated the gene regulatory mechanisms underlying the genetic associations observed at  
74 all 44 TGCT GWAS risk loci by performing *in-situ* chromosome conformation capture in TGCT cells  
75 (Hi-C) to characterize chromatin interactions between predisposition SNPs and target genes,  
76 integrating these data with a range of publicly available TGCT functional genomics data.

77

78 We conducted a new GWAS using the Oncoarray platform (3,206 UK TGCT cases/7,422 UK controls),  
79 followed by a meta-analysis combining the two largest published TGCT GWAS datasets<sup>11,16</sup> (986 UK  
80 cases/4,946 UK controls, 1,327 Scandinavian cases/6,687 Scandinavian controls) (**Fig. 1**). To increase  
81 genomic resolution, we imputed >10 million SNPs using the 1000 Genomes Project as a reference  
82 panel. Quantile-Quantile (Q-Q) plots for SNPs with minor allele frequency (MAF) >5% post  
83 imputation did not show evidence of substantive over-dispersion ( $\lambda_{1000}=1.03$ , **Supplementary Fig. 1**).  
84 We derived joint odds ratios (ORs) and 95% confidence intervals (CIs) under a fixed-effects model for  
85 each SNP with MAF >0.01. Finally we sought validation of 37 SNPs associated at  $P < 5.0 \times 10^{-6}$ , which



86 did not map to known TGCT risk loci and displayed a consistent OR across all GWAS datasets, by  
87 genotyping an additional 1,801 TGCT cases and 4,027 controls from the UK. After meta-analysis of  
88 the three GWAS and replication series, we identified genome-wide significant associations (*i.e.*  $P < 5$   
89  $\times 10^{-8}$ ) at 19 new loci (**Table 1**). We found no evidence for significant interactions between risk loci.

90 To the extent that they have been deciphered, many GWAS risk loci map to non-coding regions of  
91 the genome and influence gene regulation. Across the 44 independent TGCT risk loci (19 new and 25  
92 previously reported), we confirmed a significant enrichment of enhancer/promoter associated  
93 histone marks, including H3K4me1, H3K4me3 and H3K9ac, using available ChIP-Seq data from the  
94 TGCT cell line NTERA2 ( $P < 5.0 \times 10^{-3}$ ) (**Supplementary Table 1**). Moreover this enrichment showed  
95 tissue specificity when compared to 41 other cell lines from the ENCODE<sup>21</sup> project (**Supplementary**  
96 **Fig. 2**). These observations support the assertion that the TGCT predisposition loci influence risk  
97 through effects on *cis*-regulatory networks, and are involved in transcriptional initiation and  
98 enhancement. Since genomic spatial proximity and chromatin looping interactions are fundamental  
99 for regulation of gene expression we performed *in situ* capture Hi-C of promoters in NTERA2 cells to  
100 link risk loci to candidate target genes. We also sought to gain insight into the possible biological  
101 mechanisms for the associations by performing tissue-specific expression quantitative trait loci  
102 (eQTL) analysis for all risk SNP and target gene pairs (**Supplementary Fig. 3, Supplementary Table 2**).

103 We analysed RNA-seq data from both normal testis (GTEx project<sup>22</sup>) and TGCT (TCGA),  
104 acknowledging that the latter may be affected by the issue of tumour purity, in addition to  
105 dysregulated gene expression that typifies cancer. Accepting this limitation and that further  
106 validation may be required, eQTL analysis was conducted in both datasets based on the established  
107 network of enhancer/ promoter variants, to maximise our ability to find statistically significant  
108 associations after correcting for multiple testing. We additionally annotated risk loci with variants  
109 predicted to disrupt binding motifs of germ cell specific transcription factors (TF) (see methods).

110 Finally, direct promoter variants and non-synonymous coding mutations for genes within the 44 risk  
111 loci were denoted (**Table 2, Fig. 2**).

112

113 Although preliminary and requiring functional validation, three candidate disease mechanisms  
114 emerge from analysis across the 44 loci. Firstly, 10 of the risk loci contain candidate genes linked to  
115 developmental transcriptional regulation, as evidenced by Hi-C looping interactions (at 8p23.1,  
116 20q13.2), eQTL effects (at 4q22.3, 8p23.1), promoter variants (at 8q13.3, 9p24.3, 12q15, 17q12,  
117 19p12) and coding variants (at 2p13.3, 16q24.2) (**Table 2**). Notably the new TGCT risk locus at 8p23.1  
118 features a looping chromatin interaction from risk SNP rs17153755 to the promoter of *GATA4*, which  
119 is supported by an overlapping predicted strong enhancer region and a nominal eQTL effect (TCGA  
120 data,  $P=3.1 \times 10^{-2}$ ) (**Fig. 3a**). The rs17153755 risk allele was associated with down-regulation of  
121 *GATA4* expression, consistent with the hypothesised role of *GATA4* as a tumor suppressor gene<sup>23,24</sup>.  
122 In addition the risk locus at 16q24.2 only contains a single gene *ZFPM1* (alias FOG, Friend of GATA1),  
123 which encodes an essential regulator of *GATA1*<sup>25</sup>, in which we noted a predicted damaging<sup>26</sup>  
124 missense polymorphism (rs3751673, NP\_722520.2:p.Arg22Gly). The GATA family of transcription  
125 factors are expressed throughout postnatal testicular development<sup>27</sup>, and play a key role in ensuring  
126 correct tissue specification and differentiation<sup>28</sup>. We also observed promoter variants at 8q13.3 and  
127 9p24.3, providing support respectively for the role of *PRDM14* and *DMRT1* in TGCT oncogenesis,  
128 both of which encode important transcriptional regulators of germ cell specification and sex  
129 determination<sup>29-32</sup>. Of final note the new locus at 20q13.2 was characterized by a predicted  
130 disrupted POU5F1 binding motif, together with a looping Hi-C contact from risk SNP rs12481572 to  
131 the promoter of *SALL4*, a gene associated with the maintenance of pluripotency in embryonic stem  
132 cells<sup>33</sup>.

133 Secondly, candidate genes with roles related to microtubule/chromosomal assembly were  
134 implicated at five TGCT risk loci, supported by Hi-C looping interactions (at 1q22, 15q25.2), eQTL  
135 effects (at 15q25.2, 17q22), promoter variants (at 1q22, 4q24) and coding variants (at 21q22.3).  
136 Notably at locus 17q22 we observed a promoter variant (rs302875) which displays a strong eQTL

137 effect (GTEx data,  $P=4.9 \times 10^{-7}$ ) on *TEX14* (Testis-Expressed 14), which encodes an important  
138 regulator of kinetochore-microtubule assembly in testicular germ cells<sup>14,34,35</sup>. At new risk locus  
139 15q25.2 we identified a nominal eQTL association (rs2304416, TCGA data,  $P=3.2 \times 10^{-2}$ ) and  
140 accompanying chromatin looping interaction with mitotic spindle assembly related gene *WDR73*<sup>36</sup>  
141 (**Fig. 3b**). *WDR73* encodes a protein with a crucial role in the regulation of microtubule organization  
142 during interphase<sup>37</sup> and biallelic mutations cause Galloway-Mowat Syndrome, a human syndrome of  
143 nephrosis and neuronal dysmigration. Finally the functional analysis also highlighted microtubule  
144 assembly related genes *PMF1*, *CENPE* and *PCNT*<sup>38-41</sup> as candidates at 1q22, 4q24 and 21q22.3  
145 respectively.

146 Thirdly, the central role of KIT-MAPK signalling in TGCT oncogenesis was further supported at four  
147 loci, by Hi-C looping interactions (at 11q14.1, 15q22.31), eQTL effects (at 6p21.31) and promoter  
148 variants (at 6p21.31, 11q14.1, 15q22.31). Recent tumour sequencing studies have established that  
149 *KIT* is the major somatic driver gene for TGCT<sup>42</sup> and a relationship between the previously identified  
150 risk SNP rs995030 (12q21) and *KITLG* expression has been demonstrated through allele-specific p53  
151 binding by Zeron-Medina et al<sup>43</sup>. Here we report a new locus at 15q22.31, containing a variant within  
152 the promoter of *MAP2K1* (**Fig. 3c**), which raises the prospect of further elucidating mechanisms of  
153 KIT-MAPK signalling in driving TGCTs. *MAP2K1* (alias *MEK1*) is downstream of c-Kit and MEK1  
154 inhibition slows primordial germ cell growth in the presence of KIT ligand<sup>44</sup>. If *MAP2K1* is confirmed  
155 as a causal gene at 15q22.31, the study of somatic *KIT* mutational status in patients carrying the risk  
156 allele at 15q22.31 should be highly informative. In addition, within the 11q14.1 risk locus, we  
157 identify a candidate promoter variant for *GAB2*, which encodes a docking protein for signal  
158 transduction to MAPK and PI3K pathways which interacts directly with KIT<sup>45</sup>. Finally in our analysis  
159 we identify both a candidate promoter variant and a nominal eQTL effect for *BAK1* (6p21.31)(TCGA  
160 data,  $P=1.9 \times 10^{-2}$ ), which encodes a protein regulating apoptosis which binds with KIT<sup>40</sup>. While we  
161 have sought to decipher the functional basis of risk loci based on the cumulative weight of evidence  
162 across eQTL, Hi-C and ChIP-seq data, a limitation has been reliance on relatively small sample size for

163 eQTL analysis. Access to larger eQTL datasets in testicular tissue are likely in the future to address  
164 this deficiency enabling a better definition of the causal basis of TGCT risk at each locus.

165

166 The 44 risk loci which have now been identified for TGCT collectively account for 34% of the (father-  
167 to-son) familial risk and hence have potential clinical utility for personalized risk profiling. To assess  
168 this potential, we constructed polygenic risk scores (PRS) for TGCT, considering the combined effect  
169 of all risk SNPs modelled under a log-normal relative risk distribution. Using this approach the men in  
170 the top 1% of genetic risk have a relative risk of 14 which translates to a 7% lifetime risk of TGCT  
171 **(Supplementary Fig. 4).**

172

173 In summary, we have performed a new TGCT GWAS, identifying 19 new risk loci for TGCT,  
174 approximately doubling the number of previously reported SNPs. Using capture Hi-C we have  
175 generated a chromatin interaction map for TGCT, providing direct physical interactions between  
176 non-coding risk SNPs and target gene promoters. Moreover integration of these data together with  
177 ChIP-seq chromatin profiling and RNA-seq eQTL analysis, accepting certain caveats, has allowed us to  
178 gain preliminary but unbiased tissue-specific insight into the biological basis of TGCT susceptibility.  
179 This analysis suggests a model of TGCT susceptibility based on transcriptional dysregulation, which is  
180 likely to contribute to the developmental arrest of primordial germ cells coupled with chromosomal  
181 instability through defective microtubule function and accompanied upregulation of KIT-MAPK  
182 signalling.

183

184

185 **METHODS**

186

187 **Sample description**

188 TGCT cases were from the UK (n=5,992) and Scandinavia (n=1,327). The UK cases were ascertained  
189 from two studies (1) a UK study of familial testicular cancer and (2) a systematic collection of UK  
190 collection of TGCT cases. Case recruitment was via the UK Testicular Cancer Collaboration, a group of  
191 oncologists and surgeons treating TGCT in the UK (**Supplementary note**). The studies were co-  
192 ordinated at the Institute of Cancer Research (ICR). Samples and information were obtained with full  
193 informed consent and Medical Research and Ethics Committee approval (MREC02/06/66 and  
194 06/MRE06/41). Additional (n=1,327) case samples of Scandinavian origin were used from a  
195 previously published GWAS<sup>16</sup>.

196 Control samples for the primary GWAS were all taken from within the UK. Specifically 2,976 cancer-  
197 free, male controls were recruited through two studies within the PRACTICAL Consortium  
198 (**Supplementary note**): (1) the UK Genetic Prostate Cancer Study (UKGPCS) (age <65), a study  
199 conducted through the Royal Marsden NHS Foundation Trust and (2) SEARCH (Study of Epidemiology  
200 & Risk Factors in Cancer), recruited via GP practices in East Anglia (2003-2009). 4,446 cancer-free  
201 female controls from across the UK were recruited via the Breast Cancer Association Consortium  
202 (BCAC). Controls from the UK previously published GWAS<sup>11</sup> were from two sources within the UK:  
203 2,482 controls were from the 1958 Birth Cohort (1958BC), and 2,587 controls were identified  
204 through the UK National Blood Service (NBS) and were genotyped as part of the Wellcome Trust  
205 Case Control Consortium. Additional (n=6,687) control samples of Scandinavian origin were used in  
206 the meta-analysis, and have been previously described<sup>16</sup>. Control samples for replication genotyping  
207 (n=4,027) were taken from two studies, the national study of colorectal cancer genetics (NSCCG)<sup>46</sup>  
208 and GEnetic Lung CANcer Predisposition Study (GELCAPS)<sup>47</sup>. NSCCG and GELCAP controls were  
209 spouses of cancer patients with no personal history of cancer at time of ascertainment.

210

211 **Primary GWAS**

212 Genotyping was conducted using a custom Infinium OncoArray-500K BeadChip (Oncoarray) from  
213 Illumina (Illumina, San Diego, CA, USA), comprising a 250K SNP genome-wide backbone and 250K  
214 SNP custom content selected across multiple consortia within COGS (Collaborative Oncological  
215 Gene-environment Study). Oncoarray genotyping was conducted in accordance with the  
216 manufacturer's recommendations by the Edinburgh Clinical Research Facility, Wellcome Trust CRF,  
217 Western General Hospital, Edinburgh EH4 2XU.

218

219 **Published GWAS**

220 The UK and Scandinavian GWAS have been previously reported<sup>8,11,13</sup>. Briefly the UK GWAS comprised  
221 986 cases genotyped on the Illumina HumanCNV370-Duo bead array (Illumina, San Diego, CA, USA)  
222 and 4,946 controls genotyped on the Illumina Infinium 1.2M array. We analysed data on a common  
223 set of 314,861 SNPs successfully genotyped by both arrays. The Scandinavian GWAS<sup>16</sup>, comprised  
224 1,326 cases and 6,687 controls genotyped using the Human OmniExpressExome-8v1 Illumina array.

225

226 **Quality Control of GWAS**

227 Oncoarray data was filtered as follows, we excluded individuals with low call rate (<95%), with  
228 abnormal autosomal heterozygosity or with >10% non-European ancestry (based on multi-  
229 dimensional scaling). We filtered out all SNPs with minor allele frequency <1%, a call rate of <95% in  
230 cases or controls or with a minor allele frequency of 1–5% and a call rate of <99%, and SNPs  
231 deviating from Hardy-Weinberg equilibrium ( $10^{-12}$  in controls and  $10^{-5}$  in cases). The final number of  
232 SNPs passing quality control filters was 371,504. Quality control (QC) procedures for the UK and  
233 Scandinavian GWAS have been previously described<sup>8,11,13,16</sup>.

234

## 235 **Imputation**

236 Genome-wide imputation was performed for all GWAS datasets. The 1000 genomes phase 1 data

237 (Sept-13 release) was used as a reference panel, with haplotypes pre-phased using SHAPEIT2<sup>48</sup>.

238 Imputation was performed using IMPUTE2 software<sup>49</sup> and association between imputed genotype

239 and TGCT was tested using SNPTEST<sup>50</sup>, under a frequentist model of association. QC was performed

240 on the imputed SNPs; excluding those with INFO score < 0.8 and MAF < 0.01.

241

## 242 **Replication genotyping**

243 Replication genotyping of the 37 SNPs was performed by allele-specific KASPar allele-specific SNV

244 primers<sup>51</sup>. Genotyping was conducted by LGC Limited, Unit 1-2 Trident Industrial Estate, Pindar Road,

245 Hoddesdon, UK.

246

## 247 **Statistical Analysis**

248 Study sample size was chosen in order to achieve >50% power to detect common variants, defined

249 as MAF > 5%, OR > 1.3<sup>20</sup>. For Oncoarray data tests of association between imputed SNPs and TGCT

250 was performed under an additive genetic model in SNPTESTv2.5<sup>52</sup>, adjusting for principal

251 components. Inflation in the test statistics was observed at only modest levels,  $\lambda_{1000}=1.03$ . The

252 inflation factor  $\lambda$  was based on the 90% least-significant SNPs<sup>53</sup>. The adequacy of the case-control

253 matching and possibility of differential genotyping of cases and controls were formally evaluated

254 using Q-Q plots of test statistics (**Supplementary Fig. 1**). Population ancestry structure for the UK

255 and Scandinavian cohorts was assessed through visualisation of the first two principle components

256 (**Supplementary Fig. 5**); stable ancestral clustering was observed (**Supplementary Table 3**).

257 Statistical analysis of previously reported GWAS was performed as previously described<sup>8,11,13,16,54</sup>.  
258 Meta-analyses were performed using the fixed-effects inverse-variance method based on the  $\beta$   
259 estimates and standard errors from each study using META v1.6<sup>55</sup>. Cochran's Q-statistic to test for  
260 heterogeneity and the  $I^2$  statistic to quantify the proportion of the total variation due to  
261 heterogeneity were calculated<sup>56</sup>. For each new locus we examined evidence of departure from a log-  
262 additive (multiplicative) model, to assess any genotype specific effect. Using the Oncoarray data  
263 individual genotype data ORs were calculated for heterozygote ( $OR_{het}$ ) and homozygote ( $OR_{hom}$ )  
264 genotypes, which were compared to the per allele ORs. We tested for a difference in these 1d.f. and  
265 2d.f. logistic regression models to assess for evidence of deviation ( $P < 0.05$ ) from a log-additive  
266 model. Using Oncoarray data we examined for statistical interaction between any of the 44 TGCT  
267 predisposition loci by evaluating the effect of adding an interaction term to the regression model,  
268 adjusted for stage, using a likelihood ratio test (using a significance threshold of  $P < 2.58 \times 10^{-5}$  to  
269 account for 1,936 tests). Regional plots were generated using visPIG software<sup>57</sup> (**Supplementary Fig.**  
270 **6**). Polygenic risk scores (PRS) were constructed using the methodology of Pharoah et al<sup>58</sup>, based on  
271 a log-normal distribution  $LN(\mu, \sigma^2)$  with mean  $\mu$  and variance  $\sigma^2$  (*i.e.* relative risk is normally  
272 distributed on a logarithmic scale). The 0.5% lifetime risk of TGCT risk was based on 2014 UK data<sup>59</sup>,  
273 multiplied by relative risk to give lifetime risk per percentile of the PRS. For calculation of the  
274 proportion of TGCT genetic risk explained by the 44 loci, a father-to-son relative risk of four was  
275 used.

276

### 277 **Chromatin mark enrichment analysis**

278 To examine enrichment in specific ChIP-seq tracks across risk loci we adapted the variant set  
279 enrichment method of Cowper-Salari et al<sup>60</sup>. Briefly, for each risk locus, a region of strong LD was  
280 defined (*i.e.*  $R^2 > 0.8$  and  $D' > 0.8$ ), and SNPs mapping to these regions were termed the associated  
281 variant set (AVS). Histone ChIP-seq uniform peak data was obtained from ENCODE<sup>21</sup> for the NTERA2



282 cell line, and data was included for four histone marks. For each of these marks, the overlap of the  
283 SNPs in the AVS and the binding sites was determined to produce a mapping tally. A null distribution  
284 was produced by randomly selecting SNPs with the same LD structure as the risk associated SNPs,  
285 and the null mapping tally calculated. This process was repeated 10,000 times, and approximate *P*-  
286 values were calculated as the proportion of permutations where null mapping tally was greater or  
287 equal to the AVS mapping tally. An enrichment score was calculated by normalizing the tallies to the  
288 median of the null distribution. Thus the enrichment score is the number of standard deviations of  
289 the AVS mapping tally from the mean of the null distribution tallies. Tissue specificity was assessed  
290 by comparison of enrichment levels in NTERA2, compared to 41 other cell lines from ENCODE<sup>21</sup>, with  
291 analysis performed using the same method as above (**Supplementary Fig. 2**).

292

### 293 **Promoter Hi-C**

294 *In situ* Hi-C libraries were prepared as described by Rao et al.<sup>61</sup> with the following modifications: (i)  
295 25 million cells were fixed and processed; (ii) HindIII enzyme (NEB, Ipswich, MA, USA) was used and  
296 digestion was performed overnight; (iii) ligation was performed overnight at 16C; (iv) 3 µl of 15 µM  
297 annealed PE adaptors were ligated incubating 3 µl of T4 DNA ligase (NEB, Ipswich, MA, USA) for 2h at  
298 RT; (vi) 6 cycles of PCR were performed to amplify the libraries before capture. A Sure Select  
299 (Agilent, Santa Clara, CA, USA) custom promoter kit was used to perform capture with the same  
300 design as described by Misfud *et al.*<sup>62</sup>. For each capture reaction, 750 µg of Hi-C libraries were used.  
301 Capture was performed following the manufacture protocol and employing a custom reagent kit  
302 (Agilent, Santa Clara, CA, USA). Final PCR amplification was performed using 5 cycles to minimise PCR  
303 duplicates. 2x100bp sequencing was performed using Illumina HiSeq2000 or 2500 technology  
304 (Illumina, San Diego, CA, USA). The HiCUP pipeline<sup>63</sup> was used to process raw sequencing reads, map  
305 di-tag positions against the reference human genome and remove duplicate reads. The protocol was  
306 performed for two independent NTERA2 cell culture replicates, with cells obtained from the

307 laboratory of Prof. Janet Shipley (The Institute of Cancer Research, London) and their identity  
308 independently confirmed through STR typing at an external laboratory (Public Health England,  
309 Porton Down, UK). Cells were tested and found to be negative for mycoplasma contamination. Both  
310 Hi-C libraries achieving the following quality control thresholds: >80% reads uniquely aligning, >80%  
311 valid pair rate, >85% unique di-tag rate and >80% of interactions being *cis* (**Supplementary Table 4**).  
312 Statistically significant interactions were called using the CHiCAGO pipeline<sup>64</sup>, with both cell culture  
313 replicates processed in parallel to obtain a unique list of reproducible NTERA2 contacts. Stability of  
314 results across replicates was also verified by processing each sample individually and comparing the  
315 significance scores of called interactions; strong correlation was observed between the replicates ( $r$   
316 = 0.8,  $P < 5.0 \times 10^{-10}$ , **Supplementary Fig. 7**). Interactions with a  $-\log(\text{weighted } P\text{-value}) > 5$  were  
317 considered significant. To avoid short-range proximity bias interactions of <40kb were excluded. The  
318 distribution of interaction distances closely matched the prior published dataset of Misfud *et al.*<sup>62</sup>  
319 (**Supplementary Fig. 8**). A Hi-C track plotting read pair counts per HindIII fragment has been added  
320 to region plot figures to demonstrate the underlying signal strength of significant Hi-C contacts.

321

### 322 **3C Validation**

323 3C was used to validate selected chromatin interactions detected by Chi-C (3p24.3, 4q24, 11q14.1,  
324 15q22.31, 15q25.2, 16q12.1, and 16q23.1) (**Supplementary Fig. 9, Supplementary Table 5**). Three  
325 cell culture replicates of *in situ* 3C libraries were prepared using NTERA2 cells. Cell pellets were  
326 crosslinked, digested with HindIII, and ligated. Libraries were purified by phenol-chloroform  
327 extraction.

328 For each loci one or more bacterial artificial chromosomes (BACs; Source BioScience, Nottingham,  
329 UK) were used as an internal standard (**Supplementary Table 6**). Clones were streaked and grown  
330 before extracting DNA using a QIAGEN Plasmid Maxi Kit (QIAGEN, Hilden, Germany) which was

331 purified by phenol-chloroform extraction. In loci covered by more than one clone, equimolar  
332 solutions of clones were prepared. Randomly ligated 3C libraries were generated for each BAC or  
333 equimolar solution of BACs.

334 Unidirectional primer pairs were designed to amplify ligation junctions of the bait and other  
335 interacting HindIII fragment (promoter-element, P-E) and around the bait and a flanking control  
336 HindIII fragment in between the promoter and distal element (promoter-control, P-C) using  
337 Primer3<sup>65</sup> (**Supplementary Tables 7 and 8**). Regions were amplified using both P-E and P-C primer  
338 pairs in BAC and NTERA2 libraries using a QIAGEN Multiplex PCR Kit (QIAGEN, Hilden, Germany). 5 ng  
339 and 100 ng of BAC and NTERA2 library template DNA, respectively, were amplified using the  
340 following procedure: initial 15 minute denaturation at 95°C followed by 38 cycles of 94°C for 0.5  
341 minutes, annealing temperature specific to primer pair for 1.5 minutes seconds, 72°C extension for  
342 1.5 minutes, followed by a final 10 minute extension at 72°C extension. 5 µl of each PCR reaction  
343 was visualised on 2% agarose gels stained with ethidium bromide. ImageJ<sup>66</sup> was used to quantify  
344 intensities of PCR products and normalise for differential primer efficiency by comparing to  
345 equimolar BAC PCR products.

346 P-E fragments were Sanger sequenced in NTERA2 libraries to confirm fragments visualised on  
347 agarose gels as expected (**Supplementary Fig. 10**).

348

#### 349 **Chromatin state annotation**

350 We used ChromHMM<sup>67</sup> to infer chromatin states by integrating information on histone modifications  
351 and DNaseI hypersensitivity data to identify combinatorial and spatial patterns of epigenetic marks.  
352 Aligned next generation sequencing reads from ChIP-Seq and DNase-Seq experiments on the  
353 NTERA2 cells were downloaded from ENCODE<sup>21</sup>. Read-shift parameters for ChIP-Seq data were  
354 calculated using PHANTOMPEAKQUALTOOLS. Genome-wide signal tracks were binarised (including  
355 input controls for ChIP-Seq data) and a set of learned models were generated using ChromHMM

356 software<sup>67</sup>. The parameters of the highest scoring model were retained and model states were  
357 iteratively reduced down from 30 to 5 states. A 27-state model found to be stable and was  
358 subsequently used for segmenting the genome at 200bp resolution (**Supplementary Fig. 11**).

359

### 360 **Expression quantitative trait locus analysis**

361 We investigated for evidence of association between the SNPs at each locus and tissue specific  
362 changes in gene expression using two publically available resources: (i) RNAseq and Affymetrix 6.0  
363 SNP data for 150 TGCT patients from The Cancer Genome Atlas and (ii) normal testicular tissue data  
364 from GTEx from 157 samples<sup>22</sup>. Associations between normalized RNA counts per-gene and  
365 genotype were quantified using R package 'Matrix eQTL'. Box plots of all eQTL associations are  
366 presented in **Supplementary Fig. 3** and the tissue in which the association was observed (TGCT or  
367 normal testis), along with any other tissues resulting in a positive association, are denoted in  
368 **Supplementary Table 2**. To reduce multiple testing, association tests were only performed between  
369 SNP and gene pairs where either: (i) a direct promoter variant was observed (as per column six of  
370 **Table 2**) or (ii) a Hi-C contact to a gene promoter was observed (as per column nine of **Table 2**),  
371 together with functionally active chromatin (as per column seven of **Table 2**). The SNP used for  
372 testing at each locus was selected based on the closest available proxy (highest  $R^2$ ) to the functional  
373 variant (*i.e.* the promoter or Hi-C contact variant), rather than using the sentinel SNP with the  
374 strongest TGCT association. Finally, as a comparison all possible gene/variant eQTL combinations  
375 were also tested at each locus (ignoring the functional Hi-C/promoter/ChIP-seq data), to provide a  
376 reference overview of all possible eQTL associations at each locus (**Supplementary Table 9**).

377

### 378 **Transcription factor binding motif analysis**

379 The impact of variants on regulatory motifs was assessed for a set of transcription factors (TF)  
380 associated with germ cell development. A germ cell specific TF set was utilized, rather than all TF  
381 globally, to provide increased specificity. An OMIM<sup>68</sup> search-term-driven method was used to define  
382 the germ cell development TF set, using the following search terms: “germ cell” AND “development”  
383 AND “transcription factor” (n=46). The TF list was then intersected with predicted TF binding motifs  
384 based on a library of position weight matrices computed by Kheradpour and Kellis (2014)<sup>69 70</sup>. The  
385 intersected dataset contained motif position data for 10 TFs: DMRT1, GATA, KLF4, LHX8, NANOG,  
386 POU5F1, PRDM1, SOX2, SOX9, and CTCF. To validate the specificity of these motifs for TGCT we  
387 conducted variant set enrichment analysis, using the same method as detailed above (based on  
388 Cowper-Salari *et al*<sup>60</sup>), which confirmed enrichment for disruption of these 10 motifs in the 44 TGCT  
389 risk loci compared to the null distribution (**Supplementary Table 10**).

390

### 391 **Integration of functional data**

392 For the integrated functional annotation of risk loci LD blocks were defined as all SNPs in  $R^2 > 0.8$   
393 with the sentinel SNP. Risk loci were then annotated with six types of functional data: (i) presence of  
394 a Hi-C contact linking to a gene promoter, (ii) presence of an expression quantitative trait locus, (iii)  
395 presence of a ChIP-seq peak, (iv) presence of a disrupted transcription factor binding motif, (v)  
396 presence of a variant within a gene promoter boundary, with boundaries defined using the Ensembl  
397 regulatory build<sup>71</sup>, (vi) presence of a non-synonymous coding change. Candidate causal genes were  
398 then assigned to TGCT risk loci using the target genes implicated in annotation tracks (i), (ii), (v) and  
399 (vi). Where the data supported multiple gene candidates, the gene with the highest number of  
400 individual functional data points was assigned to be the candidate. Where multiple genes have the  
401 same number of data points all genes are listed. Direct non-synonymous coding variants were  
402 allocated additional weighting. Competing mechanisms for the same gene (e.g. both coding and  
403 promoter variants) were allowed.

404

405 **ACKNOWLEDGEMENTS**

406 We thank the subjects with TGCT and the clinicians involved in their care for participation in this  
407 study. We thank the patients and all clinicians forming part of the UK Testicular Cancer Collaboration  
408 (UKTCC) for their participation in this study. A full list of UKTCC members is included in  
409 **Supplementary note**. We acknowledge National Health Service funding to the National Institute for  
410 Health Research Biomedical Research Centre. We thank the UK Genetics of Prostate Cancer Study  
411 (UKGPCS) study teams for the recruitment of the UKGPCS controls. Genotyping of the OncoArray  
412 was funded by the US National Institutes of Health (NIH) [U19 CA 148537 for ELucidating Loci  
413 Involved in Prostate cancer SuscEptibility (ELLIPSE) project and X01HG007492 to the Center for  
414 Inherited Disease Research (CIDR) under contract number HHSN268201200008I]. Additional analytic  
415 support was provided by NIH NCI U01 CA188392 (PI: Schumacher). The PRACTICAL consortium was  
416 supported by Cancer Research UK Grants C5047/A7357, C1287/A10118, C1287/A16563,  
417 C5047/A3354, C5047/A10692, C16913/A6135, European Commission's Seventh Framework  
418 Programme grant agreement n° 223175 (HEALTH-F2-2009-223175), and The National Institute of  
419 Health (NIH) Cancer Post-Cancer GWAS initiative grant: No. 1 U19 CA 148537-01 (the GAME-ON  
420 initiative). A full list of PRACTICAL consortium members is included in **Supplementary note**. We  
421 would also like to thank the following for funding support: The Institute of Cancer Research and The  
422 Everyman Campaign, The Prostate Cancer Research Foundation, Prostate Research Campaign UK  
423 (now Prostate Action), The Orchid Cancer Appeal, The National Cancer Research Network UK, The  
424 National Cancer Research Institute (NCRI) UK. We are grateful for support of NIHR funding to the  
425 NIHR Biomedical Research Centre at The Institute of Cancer Research and The Royal Marsden NHS  
426 Foundation Trust. This study would not have been possible without the contributions of the  
427 following: M. K. Bolla (BCAC), Q. Wang (BCAC), K. Michailido (BCAC), J. Dennis (BCAC), P. Hall (COGS);  
428 D.F. Easton (BCAC), A. Berchuck (OCAC), R. Eeles (PRACTICAL), G. Chenevix-Trench (CIMBA), J.  
429 Dennis, P. Pharoah, A. Dunning, K. Muir, J. Peto, A. Lee, and E. Dicks. We also thank the following for

430 their contributions to this project: Jacques Simard, Peter Kraft, Craig Luccarini and the staff of the  
431 Centre for Genetic Epidemiology Laboratory; and Kimberly F. Doheny and the staff of the Center for  
432 Inherited Disease Research (CIDR) genotyping facility. The results published here are in part based  
433 upon data generated by the TCGA Research Network: <http://cancergenome.nih.gov/>. This study  
434 makes use of data generated by the Wellcome Trust Case Control Consortium 2 (WTCCC2). A full list  
435 of the investigators who contributed to the generation of the data is available from the WTCCC  
436 website. We acknowledge the contribution of Elizabeth Rapley and Mike Stratton to the generation  
437 of previously published UK GWAS case data. We acknowledge funding from the Swedish Cancer  
438 Society (CAN2011/484 and CAN2012/823), the Norwegian Cancer Society (grants number 418975 –  
439 71081 – PR-2006-0387 and PK01-2007-0375) and the Nordic Cancer Union (grant number S-12/07).  
440 This study was supported by the Movember foundation and the Institute of Cancer Research. K.  
441 Litchfield is supported by a PhD fellowship from Cancer Research UK. R.S.H. and P.B. are supported  
442 by Cancer Research UK (C1298/A8362 Bobby Moore Fund for Cancer Research UK). We thank all the  
443 individuals who took part in these studies and all the researchers, clinicians, technicians and  
444 administrative staff who have enabled this work to be carried out.

445

#### 446 **AUTHOR CONTRIBUTIONS**

447 C.T., K.L., and R.S.H designed the study. Case samples were recruited by A.R., R.H. and through  
448 UKTCC. R.E., A.D, K.M, J.P., Z.K-J, N.P. and D.E supplied Oncoarray control data. N.O. administrated  
449 genotyping of Oncoarray case samples. D.D. coordinated all case sample administration and  
450 tracking. K.L., M.L., A.H. and P.B. prepared samples for genotyping experiments. K.L., M.L., G.O., C.L.,  
451 K.F. and I.A. conducted all Promotor HiC and 3C laboratory experiments. Bioinformatics and  
452 statistical analyses were designed by C.T., R.S.H and K.L.. K.L., G.M., C.L. and M.L. conducted all  
453 Promotor HiC and 3C data analysis. K.L. and P.L. conducted transcription factor enrichment analysis.  
454 K. L., C.L. and M.L. performed all other bioinformatics and statistical analyses. R.K., T. H., W. K., T.G.

455 and F.W. provided Scandinavian GWAS data. K. L. drafted the manuscript with assistance from C.T.,  
456 R.S.H., M.L., J.S., J.N. and T.B. All authors reviewed and contributed to the manuscript.

457

#### 458 **DATA AVAILABILITY**

459 Case Oncoarray GWAS data and the Hi-C dataset utilized in this paper have both been deposited in  
460 the European Genome–phenome Archive (EGA), which is hosted by the European Bioinformatics  
461 Institute (EBI), under the accession codes EGAS00001001836 and EGAS00001001930 respectively.

462

#### 463 **COMPETING FINANCIAL INTERESTS**

464 The authors declare no competing financial interests.

465

#### 466 **FIGURES AND TABLE LEGENDS**

467 **Figure 1 - Study design.**

468 **Figure 2 - Circos plot of integrated functional analysis for all 44 TGCT risk loci.** Inner-most ring  
469 represents the presence of a Hi-C contact in the NTERA2 cell line, the next four rings are narrow-  
470 peak histone ChIP-seq tracks for NTERA2, the sixth ring represents  $-\log P$  values of TGCT risk  
471 association from the Oncoarray GWAS data with green line denoting genome-wide significance and  
472 the seventh ring (outer-most) is the functional annotation and classification of candidate causal  
473 genes.

474 **Figure 3A-C – Regional plots of three new TGCT loci at A) 8p23.1, B) 15q25.2 and C) 15q22.31.**  
475 Shown by triangles are the  $-\log_{10}$  association P values of genotyped SNPs, based on Oncoarray data.  
476 Shown by circles are imputed SNPs at each locus. The intensity of red shading indicates the strength  
477 of LD with the sentinel SNP (labelled). Also shown are the SNP build 37 coordinates in mega-bases,  
478 recombination rates in centi-morgans (in light blue) and the genes in the region. Below the gene  
479 transcripts are Hi-C next generation sequencing read pair counts (gaps represent bait locations) and  
480 significant Hi-C interactions. Below the axis is a zoomed-in section displaying the surrounding genes  
481 for each SNP, the predicted chromHMM states along with an arc depiction of the same Hi-C  
482 contact(s).

483



**Table 1 - Summary of genotyping results for all genome-wide TGCT risk SNPs (n=44). New loci (n=19) discovered through this study are marked in bold.**

SNP <sup>1</sup>	Chr.	Pos. (b37)	Alleles <sup>2</sup>	RAF <sup>3</sup>	Oncoarray		Discovery Meta		Replication		Combined-Meta	
					OR <sup>4</sup> (95% CI)	Ptrend <sup>5</sup>	OR (95% CI)	Ptrend	OR (95% CI)	Ptrend	P meta <sup>6</sup>	(I <sup>2</sup> ) <sup>7</sup>
<b>rs4240895</b>	<b>1</b>	<b>9713386</b>	<b>C/T</b>	<b>0.39</b>	<b>1.13 (1.07-1.19)</b>	<b>7.8X10-05</b>	<b>1.14 (1.09-1.19)</b>	<b>1.7X10-07</b>	<b>1.24 (1.16-1.32)</b>	<b>1.7X10-07</b>	<b>6.2X10-13</b>	<b>47</b>
rs2072499	1	156169610	A/G	0.36	1.14 (1.08-1.20)	2.2X10-05	1.18 (1.13-1.23)	1.9X10-10	-	-	1.9X10-10	45
rs3790672	1	165873392	T/C	0.29	1.16 (1.10-1.23)	3.7X10-06	1.20 (1.14-1.25)	5.3X10-11	-	-	5.3X10-11	17
<b>rs7581030</b>	<b>2</b>	<b>71572455</b>	<b>C/T</b>	<b>0.24</b>	<b>1.15 (1.08-1.22)</b>	<b>5.9X10-05</b>	<b>1.17 (1.12-1.23)</b>	<b>8.3X10-09</b>	<b>1.17 (1.08-1.26)</b>	<b>6.2X10-04</b>	<b>2.1X10-11</b>	<b>0</b>
rs10510452	3	16625048	A/G	0.70	1.15 (1.08-1.21)	2.4X10-05	1.18 (1.13-1.23)	9.5X10-10	-	-	9.5X10-10	43
rs11705932	3	141818850	C/T	0.80	1.18 (1.11-1.26)	1.1X10-05	1.17 (1.11-1.23)	4.5X10-07	-	-	4.5X10-07	39
rs1510272	3	156300724	C/T	0.75	1.19 (1.12-1.26)	4.8X10-07	1.23 (1.17-1.28)	1.7X10-12	-	-	1.7X10-12	33
<b>rs6821144</b>	<b>4</b>	<b>76520651</b>	<b>G/A</b>	<b>0.89</b>	<b>1.18 (1.08-1.27)</b>	<b>9.7X10-04</b>	<b>1.22 (1.14-1.30)</b>	<b>1.9X10-06</b>	<b>1.35 (1.23-1.47)</b>	<b>9.8X10-07</b>	<b>2.3X10-11</b>	<b>18</b>
rs17021463	4	95224812	T/G	0.43	1.14 (1.09-1.20)	6.4X10-06	1.14 (1.10-1.19)	3.3X10-08	-	-	3.3X10-08	0
rs2720460	4	104054686	A/G	0.63	1.24 (1.18-1.31)	2.2X10-12	1.26 (1.21-1.31)	6.6X10-20	-	-	6.6X10-20	10
<b>rs4862848</b>	<b>4</b>	<b>188921440</b>	<b>A/G</b>	<b>0.35</b>	<b>1.18 (1.10-1.25)</b>	<b>1.2X10-05</b>	<b>1.21 (1.16-1.27)</b>	<b>3.5X10-12</b>	<b>1.10 (1.02-1.18)</b>	<b>2.4X10-02</b>	<b>1.9X10-12</b>	<b>61</b>
rs2736100	5	1286516	C/A	0.51	1.25 (1.19-1.30)	2.5X10-13	1.28 (1.24-1.33)	9.0X10-25	-	-	9.0X10-25	27
rs3805663	5	134342720	C/A	0.58	1.09 (1.03-1.15)	6.0X10-03	1.12 (1.07-1.17)	1.2X10-05	-	-	1.2X10-05	20
rs4624820	5	141681788	G/A	0.56	1.46 (1.40-1.52)	3.8X10-36	1.47 (1.43-1.52)	2.5X10-57	-	-	2.5X10-57	0
rs210138	6	33542538	A/G	0.21	1.42 (1.35-1.49)	1.0X10-21	1.48 (1.42-1.54)	3.5X10-37	-	-	3.5X10-37	70
<b>rs11155671</b>	<b>6</b>	<b>149972132</b>	<b>G/A</b>	<b>0.66</b>	<b>1.16 (1.09-1.22)</b>	<b>6.1X10-06</b>	<b>1.15 (1.10-1.20)</b>	<b>1.9X10-07</b>	<b>1.14 (1.05-1.22)</b>	<b>3.3X10-03</b>	<b>2.3X10-09</b>	<b>0</b>
rs12699477	7	1968953	T/C	0.39	1.22 (1.16-1.28)	1.1X10-10	1.20 (1.15-1.25)	5.9X10-13	-	-	5.9X10-13	0
<b>rs17689040</b>	<b>7</b>	<b>40920313</b>	<b>C/G</b>	<b>0.43</b>	<b>1.15 (1.10-1.21)</b>	<b>2.1X10-06</b>	<b>1.15 (1.10-1.19)</b>	<b>5.6X10-08</b>	<b>1.17 (1.09-1.25)</b>	<b>1.2X10-04</b>	<b>3.1X10-11</b>	<b>0</b>
<b>rs17153755</b>	<b>8</b>	<b>11611500</b>	<b>C/G</b>	<b>0.65</b>	<b>1.19 (1.13-1.25)</b>	<b>1.6X10-08</b>	<b>1.16 (1.11-1.21)</b>	<b>1.5X10-08</b>	<b>1.05 (0.97-1.14)</b>	<b>2.8X10-01</b>	<b>4.4X10-08</b>	<b>68</b>
rs7010162	8	70976505	C/T	0.62	1.13 (1.07-1.19)	7.6X10-05	1.15 (1.10-1.20)	4.5X10-08	-	-	4.5X10-08	0
rs7040024	9	845516	A/C	0.77	1.48 (1.41-1.55)	2.3X10-27	1.53 (1.47-1.59)	2.2X10-45	-	-	2.2X10-45	42
rs7107174	11	77996403	C/A	0.22	1.19 (1.11-1.27)	2.6X10-05	1.17 (1.10-1.24)	5.3X10-06	-	-	5.3X10-06	0
<b>rs648090</b>	<b>11</b>	<b>125071163</b>	<b>A/G</b>	<b>0.71</b>	<b>1.18 (1.12-1.25)</b>	<b>4.7X10-07</b>	<b>1.15 (1.10-1.20)</b>	<b>7.6X10-08</b>	<b>1.24 (1.15-1.33)</b>	<b>2.4X10-06</b>	<b>2.2X10-12</b>	<b>24</b>
rs2900333	12	14653867	C/T	0.63	1.17 (1.11-1.23)	3.7X10-07	1.20 (1.15-1.25)	9.3X10-13	-	-	9.3X10-13	17
<b>rs4931000</b>	<b>12</b>	<b>32141495</b>	<b>A/G</b>	<b>0.22</b>	<b>1.16 (1.09-1.23)</b>	<b>3.4X10-05</b>	<b>1.16 (1.11-1.22)</b>	<b>1.2X10-07</b>	<b>1.23 (1.13-1.32)</b>	<b>2.3X10-05</b>	<b>1.9X10-11</b>	<b>0</b>
<b>rs7315956</b>	<b>12</b>	<b>70563865</b>	<b>A/G</b>	<b>0.34</b>	<b>1.13 (1.06-1.19)</b>	<b>2.0X10-04</b>	<b>1.13 (1.08-1.18)</b>	<b>6.5X10-07</b>	<b>1.16 (1.08-1.25)</b>	<b>2.9X10-04</b>	<b>8.7X10-10</b>	<b>0</b>
rs3782181	12	88953561	C/A	0.81	2.06 (1.99-2.14)	1.4X10-80	2.07 (2.01-2.12)	3.3X10-129	-	-	3.3X10-129	40
<b>rs1009647</b>	<b>14</b>	<b>55880047</b>	<b>G/A</b>	<b>0.73</b>	<b>1.13 (1.06-1.19)</b>	<b>4.1X10-04</b>	<b>1.15 (1.10-1.21)</b>	<b>5.9X10-07</b>	<b>1.12 (1.03-1.21)</b>	<b>1.7X10-02</b>	<b>3.4X10-08</b>	<b>0</b>
<b>rs11071896</b>	<b>15</b>	<b>66821250</b>	<b>A/G</b>	<b>0.26</b>	<b>1.17 (1.10-1.24)</b>	<b>4.9X10-06</b>	<b>1.19 (1.14-1.25)</b>	<b>9.2X10-10</b>	<b>1.18 (1.09-1.27)</b>	<b>2.1X10-04</b>	<b>8.4X10-13</b>	<b>0</b>
<b>rs56046484</b>	<b>15</b>	<b>85605427</b>	<b>G/T</b>	<b>0.80</b>	<b>1.17 (1.09-1.24)</b>	<b>4.5X10-05</b>	<b>1.17 (1.11-1.23)</b>	<b>2.7X10-07</b>	<b>1.11 (1.01-1.21)</b>	<b>3.8X10-02</b>	<b>4.6X10-08</b>	<b>0</b>
rs4561483	16	11920037	A/G	0.35	1.11 (1.05-1.17)	1.1X10-03	1.13 (1.08-1.18)	5.5X10-07	-	-	5.5X10-07	3
<b>rs7404843</b>	<b>16</b>	<b>15530708</b>	<b>T/G</b>	<b>0.11</b>	<b>1.21 (1.12-1.30)</b>	<b>4.7X10-05</b>	<b>1.28 (1.21-1.35)</b>	<b>1.1X10-11</b>	<b>1.17 (1.05-1.29)</b>	<b>9.8X10-03</b>	<b>7.9X10-13</b>	<b>42</b>
rs8046148	16	50142944	A/G	0.79	1.10 (1.03-1.17)	7.8X10-03	1.16 (1.10-1.21)	4.5X10-07	-	-	4.5X10-07	58
rs4888262	16	74670458	C/T	0.50	1.17 (1.11-1.23)	1.2X10-07	1.18 (1.13-1.23)	6.9X10-12	-	-	6.9X10-12	0
rs55637647	16	88549264	C/G	0.38	1.15 (1.09-1.22)	7.2X10-06	1.17 (1.12-1.22)	2.9X10-09	-	-	2.9X10-09	0

rs7501939	17	36101156	T/C	0.61	1.22 (1.16-1.28)	7.8X10-11	1.25 (1.21-1.30)	2.8X10-20	-	-	2.8X10-20	55
rs9905704	17	56632543	G/T	0.68	1.27 (1.20-1.33)	2.4X10-13	1.27 (1.22-1.32)	3.4X10-20	-	-	3.4X10-20	0
rs9966612	<b>18</b>	<b>649311</b>	<b>A/G</b>	<b>0.32</b>	<b>1.16 (1.08-1.23)</b>	<b>9.8X10-05</b>	<b>1.17 (1.12-1.23)</b>	<b>2.1X10-08</b>	<b>1.13 (1.05-1.22)</b>	<b>5.1X10-03</b>	<b>4.4X10-10</b>	<b>0</b>
rs2195987	19	24149545	C/T	0.83	1.18 (1.08-1.28)	1.3X10-03	1.22 (1.15-1.28)	9.9X10-09	-	-	9.9X10-09	0
rs2241024	<b>19</b>	<b>28257393</b>	<b>G/A</b>	<b>0.80</b>	<b>1.24 (1.17-1.31)</b>	<b>4.7X10-09</b>	<b>1.23 (1.16-1.29)</b>	<b>1.4X10-10</b>	<b>1.32 (1.22-1.42)</b>	<b>6.3X10-08</b>	<b>1.0X10-16</b>	<b>29</b>
rs4599029	19	54284689	G/T	0.74	1.18 (1.11-1.25)	1.1X10-06	1.16 (1.11-1.22)	7.6X10-08	1.10 (1.01-1.19)	3.8X10-02	1.4X10-08	19
rs12481572	<b>20</b>	<b>50708054</b>	<b>A/T</b>	<b>0.20</b>	<b>1.20 (1.13-1.28)</b>	<b>9.5X10-07</b>	<b>1.20 (1.14-1.27)</b>	<b>1.4X10-08</b>	<b>1.23 (1.13-1.33)</b>	<b>3.7X10-05</b>	<b>2.5X10-12</b>	<b>0</b>
rs2839186	21	47690068	C/T	0.48	1.17 (1.11-1.23)	1.6X10-07	1.18 (1.14-1.23)	7.1X10-12	-	-	7.1X10-12	0
rs739525	<b>22</b>	<b>21332441</b>	<b>T/C</b>	<b>0.53</b>	<b>1.13 (1.06-1.19)</b>	<b>1.8X10-04</b>	<b>1.14 (1.09-1.19)</b>	<b>2.0X10-07</b>	<b>1.10 (1.02-1.18)</b>	<b>2.2X10-02</b>	<b>1.9X10-08</b>	<b>0</b>

485

486 <sup>1</sup> dbSNP rs number487 <sup>2</sup> Alleles488 <sup>3</sup> Risk Allele Frequency489 <sup>4</sup> OR: per allele odds ratio490 <sup>5</sup>  $P_{trend}$ :  $P$ -value for trend, via logistic regression491 <sup>6</sup>  $P_{meta}$ :  $P$ -value for fixed effects meta-analysis492 <sup>7</sup>  $I^2$  heterogeneity index (0-100)

493

494 **Table 2 – Summary of functional annotation of all 44 TGCT risk loci.** Novel risk loci are highlighted in bold.

SNP	Cyto-band	bp (b37)	Genes in LD Block	Functional Evidence							Candidate causal Gene(s)	Functional Pathway
				Coding Variant	Promoter Variant	Functional Chromatin (ChIP-seq peaks)	TF binding motif disruption	Hi-C Contact(s)	eQTL	Functional Study		
rs4240895	<b>1p36.22</b>	<b>9,713,386</b>	<b>PIK3CD C1orf200</b>				KLF4					
rs2072499	1q22	156,169,610	KIAA0446 SLC25A44		PMF1	H3k4me1, H3k4me3, H3k9ac	PRDM1, CTCF	BGLAP, CCT3, PAQR6, PMF1, SEMA4A, UBQLN4	CCT3 <sup>1</sup>		PMF1  CCT3	Microtubule/ chromosomal assembly
rs3790672	1q24.1	165,873,392	UCK2				GATA, NANOG, LHX8,					

							POU5F1, SOX9, PRDM1, CTCF					
rs7581030	2p13.3	71,572,455	ZNF638	ZNF638		H3k4me3, H3k9ac	NANOG, POU5F1	PAIP2B			ZNF638	Transcriptional Regulation
rs10510452	3p24.3	16,625,048	DAZL				GATA, NANOG, POU5F1	OXNAD1			OXNAD1	
rs11705932	3q23	141,818,850	TFDP2									
rs1510272	3q25.31	156,300,724					GATA, POU5F1, CTCF					
rs6821144	4q21.1	76,520,651	CDKL2 G3BP2			H3k4me3, H3k9ac	SOX2	G3BP2			G3BP2	
rs17021463	4q22.3	95,224,812	SMARCAD1 HPGDS	SMARCAD1	SMARCAD1	H3k4me3, H3k9ac	GATA, KLF4, NANOG, POU5F1, PRDM1	ATOH1	SMARCAD1 <sup>2</sup> ATOH1 <sup>2</sup>		SMARCAD1	Transcriptional Regulation
rs2720460	4q24	104,054,686	CENPE		CENPE	H3k4me3, H3k9ac	GATA, NANOG, LHX8, POU5F1, DMRT1	MANBA, NFKB1, SLC39A8, TACR3	MANBA <sup>2</sup>		CENPE MANBA	Microtubule/ chromosomal assembly
rs4862848	4q35.2	188,921,440	ZFP42			H3k4me3, H3k9ac						
rs2736100	5p15.33	1,286,516	TERT									
rs3805663	5q31.1	134,366,200	CATSPER3 PITX1 AK026965			H3k4me3, H3k9ac						
rs4624820	5q31.3	141,681,788	SPRY4									
rs210138	6p21.31	33,542,538	BAK1 AY383626 C6orf227		BAK1	H3k4me3, H3k9ac		GRM4	BAK1 <sup>2</sup>		BAK1	KIT-MAPK

rs11155671	6q25.1	149,972,132	KATNA1 LATS1				GATA, KLF4, NANOG, SOX2, POU5F1, DMRT1, SOX9, PRDM1, CTCF					
rs12699477	7p22.3	1,968,953	MAD1L1			H3k4me1, H3k9ac	NANOG, CTCF					
rs17689040	7p14.1	40,920,313										
rs17153755	8p23.1	11,611,500	GATA4 c8orf			H3k4me3, H3k9ac	CTCF	GATA4	GATA4 <sup>2</sup>		GATA4	Transcriptional Regulation
rs7010162	8q13.3	70,976,505	PRDM14		PRDM14		GATA, PRDM1				PRDM14	Transcriptional Regulation
rs7040024	9p24.3	845,516	DMRT1		DMRT1	H3k4me3, H3k9ac	GATA, KLF4, CTCF				DMRT1	Transcriptional Regulation
rs7107174	11q14.1	77,997,936	GAB2	USP35	GAB2	H3k4me3, H3k9ac	GATA, KLF4, NANOG, LHX8, SOX2, POU5F1, DMRT1, SOX9, PRDM1, CTCF	ALG8, GAB2, NARS2			GAB2	KIT-MAPK
											USP35	
rs648090	11q24.2	125,071,163	PKNOX2			H3k4me1	CTCF					
rs2900333	12p13.1	14,653,867	ATF7IP PLBD1	ATF7IP	ATF7IP		GATA, NANOG, SOX2, POU5F1, CTCF				ATF7IP	Telomerase Function
rs4931000	12p11.21	32,141,495	C12orf35	KIAA1551			NANOG, CTCF				KIAA1551	
rs7315956	12q15	70,563,865	CNOT2 KCNMB4		CNOT2		GATA, NANOG, LHX8, SOX2				CNOT2	Transcriptional Regulation

rs3782181	12q21.32	88,953,561	<i>KITLG</i>			H3k4me3, H3k9ac	GATA, NANOG, SOX2, POU5F1, DMRT1, PRDM1, CTCF			<i>KITLG</i>	<i>KITLG</i>	<b>KIT-MAPK</b>
rs1009647	14q22.3	55,880,047	<i>ATG14</i> <i>DLGAP5</i> <i>FBXO34</i> <i>LGALS3</i> <i>TBPL2</i>		<i>ATG14</i>				<i>ATG14</i> <sup>1</sup>		<i>ATG14</i>	<b>Autophagy</b>
rs11071896	15q22.31	66,821,250	<i>MAP2K1</i> <i>TIPIN</i>	<i>ZWILCH</i>	<i>MAP2K1</i>	H3k4me1, H3k4me3, H3k9ac	GATA, NANOG, SOX2, DMRT1, SOX9, PRDM1, CTCF	<i>DENND4A</i> , <i>IGDCC4</i> , <i>LCTL</i> , <i>MAP2K1</i> , <i>RAB11A</i> , <i>RPL4</i> , <i>SCARNA14</i> , <i>SNAPC5</i>	<i>SNAPC5</i> <sup>2</sup>		<i>MAP2K1</i>	<b>KIT-MAPK</b>
											<i>SNAPC5</i>	
rs56046484	15q25.2	85,605,427	<i>PDE8A</i> <i>SLC28A1</i>				GATA, NANOG, LHX8, CTCF	<i>SLC28A1</i> , <i>WDR73</i>	<i>WDR73</i> <sup>2</sup>		<i>WDR73</i>	<b>Microtubule/ chromosomal assembly</b>
rs4561483	16p13.13	11,920,037	<i>BCAR4</i> <i>CATX-11</i> <i>RSL1D1</i>				KLF4, NANOG, CTCF	<i>LITAF</i>	<i>GSPT1</i> <sup>3</sup>		<i>GSPT1</i>	<b>Cell cycle</b>
rs7404843	16p13.11	15,530,708	<i>MPV17L</i>				GATA, POU5F1, CTCF					
rs8046148	16q12.1	50,142,944	<i>HEATR3</i> <i>AF086132</i>		<i>HEATR3</i>	H3k4me1, H3k4me3, H3k9ac	GATA, SOX2, CTCF	<i>HEATR3</i>	<i>HEATR3</i> <sup>1</sup>		<i>HEATR3</i>	
rs4888262	16q23.1	74,670,458	<i>RFWD3</i>		<i>RFWD3</i>	H3k4me1, H3k4me3, H3k9ac	GATA, KLF4, NANOG, PRDM1	<i>CLEC18C</i> , <i>LDHD</i> , <i>RFWD3</i> , <i>WDR59</i>	<i>RFWD3</i> <sup>1</sup>		<i>RFWD3</i>	<b>Apoptosis/p53 pathway</b>
rs55637647	16q24.2	88,549,264	<i>ZFPM1</i>	<i>ZFPM1</i>		H3k4me1, H3k9ac	KLF4				<i>ZFPM1</i>	<b>Transcriptional Regulation</b>

rs7501939	17q12	36,101,156	<i>HNFB1B</i>		<i>HNFB1B</i>	H3k4me3, H3k9ac	GATA, NANOG, SOX2, POU5F1, SOX9			<i>HNFB1B</i>	Transcriptional Regulation
rs9905704	17q22	56,632,543	<i>TEX14</i>		<i>TEX14</i>		GATA, SOX2, DMRT1, SOX9		<i>TEX14</i> <sup>1</sup>	<i>TEX14</i>	Microtubule/ chromosomal assembly
rs9966612	18p11.32	649,311	<i>CLUL1</i> <i>ENOSF1</i> <i>TYMS</i>					<i>THOC1</i>		<i>THOC1</i>	Apoptosis/p53 pathway
rs2195987	19p12	24,149,545	<i>AK125686</i>		<i>ZNF254</i>	H3k4me3, H3k9ac	SOX2, POU5F1			<i>ZNF254</i>	Transcriptional Regulation
rs2241024	19q11	28,257,393									
rs4599029	19q13.42	54,284,689	<i>NLRP12</i>				GATA, KLF4, NANOG				
rs12481572	20q13.2	50,708,054					POU5F1	<i>NFATC2</i> , <i>SALL4</i>		<i>SALL4</i>	Transcriptional Regulation
rs2839186	21q22.3	47,690,068	<i>MCM3APAS</i> <i>MCM3AP</i>	<i>C21orf58</i> , <i>PCNT</i>		H3k4me1, H3k4me3, H3k9ac	KLF4, NANOG, DMRT1, CTCF			<i>PCNT</i>	Microtubule/ chromosomal assembly
rs739525	22q11.21	21,332,441	<i>AIFM3</i>		<i>AIFM3</i>	H3k4me1, H3k4me3, H3k9ac	NANOG			<i>AIFM3</i>	Apoptosis/p53 pathway

<sup>1</sup> Significant vs threshold corrected for 96 multiple tests

<sup>2</sup> Nominally significant at P<0.05, see supplementary table 9 for exact P-values

<sup>3</sup> eQTL identified in previous study

495 **REFERENCES**

496

- 497 1. Manku, G. *et al.* Changes in the expression profiles of claudins during gonocyte  
498 differentiation and in seminomas. *Andrology* **4**, 95-110 (2016).
- 499 2. Le Cornet, C. *et al.* Testicular cancer incidence to rise by 25% by 2025 in Europe? Model-  
500 based predictions in 40 countries using population-based registry data. *Eur J Cancer* **50**, 831-  
501 9 (2014).
- 502 3. Litchfield, K. *et al.* Quantifying the heritability of testicular germ cell tumour using both  
503 population-based and genomic approaches. *Sci Rep* **5**, 13889 (2015).
- 504 4. Swerdlow, A.J., De Stavola, B.L., Swanwick, M.A. & Maconochie, N.E. Risks of breast and  
505 testicular cancers in young adult twins in England and Wales: evidence on prenatal and  
506 genetic aetiology. *Lancet* **350**, 1723-8 (1997).
- 507 5. McGlynn, K.A., Devesa, S.S., Graubard, B.I. & Castle, P.E. Increasing incidence of testicular  
508 germ cell tumors among black men in the United States. *J Clin Oncol* **23**, 5757-61 (2005).
- 509 6. Hemminki, K. & Li, X. Familial risk in testicular cancer as a clue to a heritable and  
510 environmental aetiology. *British Journal of Cancer* **90**, 1765-1770 (2004).
- 511 7. Kharazmi, E. *et al.* Cancer Risk in Relatives of Testicular Cancer Patients by Histology Type  
512 and Age at Diagnosis: A Joint Study from Five Nordic Countries. *Eur Urol* **68**, 283-9 (2015).
- 513 8. Rapley, E.A. *et al.* A genome-wide association study of testicular germ cell tumor. *Nat Genet*  
514 **41**, 807-10 (2009).
- 515 9. Turnbull, C. & Rahman, N. Genome-wide association studies provide new insights into the  
516 genetic basis of testicular germ-cell tumour. *Int J Androl* **34**, e86-96; discussion e96-7 (2011).
- 517 10. Kanetsky, P.A. *et al.* Common variation in KITLG and at 5q31.3 predisposes to testicular germ  
518 cell cancer. *Nat Genet* **41**, 811-5 (2009).
- 519 11. Turnbull, C. *et al.* Variants near DMRT1, TERT and ATF7IP are associated with testicular germ  
520 cell cancer. *Nat Genet* **42**, 604-7 (2010).
- 521 12. Kanetsky, P.A. *et al.* A second independent locus within DMRT1 is associated with testicular  
522 germ cell tumor susceptibility. *Hum Mol Genet* **20**, 3109-17 (2011).
- 523 13. Ruark, E. *et al.* Identification of nine new susceptibility loci for testicular cancer, including  
524 variants near DAZL and PRDM14. *Nat Genet* **45**, 686-9 (2013).
- 525 14. Bojesen, S.E. *et al.* Multiple independent variants at the TERT locus are associated with  
526 telomere length and risks of breast and ovarian cancer. *Nat Genet* **45**, 371-84, 384e1-2  
527 (2013).
- 528 15. Chung, C.C. *et al.* Meta-analysis identifies four new loci associated with testicular germ cell  
529 tumor. *Nat Genet* **45**, 680-5 (2013).
- 530 16. Kristiansen, W. *et al.* Two new loci and gene sets related to sex determination and cancer  
531 progression are associated with susceptibility to testicular germ cell tumor. *Hum Mol Genet*  
532 (2015).
- 533 17. Litchfield, K. *et al.* Multi-stage genome-wide association study identifies new susceptibility  
534 locus for testicular germ cell tumour on chromosome 3q25. *Hum Mol Genet* **24**, 1169-76  
535 (2015).
- 536 18. Litchfield, K. *et al.* Identification of four new susceptibility loci for testicular germ cell  
537 tumour. *Nat Commun* **6**, 8690 (2015).
- 538 19. Litchfield, K., Shipley, J. & Turnbull, C. Common variants identified in genome-wide  
539 association studies of testicular germ cell tumour: an update, biological insights and clinical  
540 application. *Andrology* **3**, 34-46 (2015).
- 541 20. Skol, A.D., Scott, L.J., Abecasis, G.R. & Boehnke, M. Joint analysis is more efficient than  
542 replication-based analysis for two-stage genome-wide association studies (vol 38, pg 209,  
543 2006). *Nature Genetics* **38**, 390-390 (2006).

- 544 21. Consortium, E.P. *et al.* An integrated encyclopedia of DNA elements in the human genome. *Nature* **489**, 57-74 (2012).
- 545
- 546 22. Consortium, G.T. The Genotype-Tissue Expression (GTEx) project. *Nat Genet* **45**, 580-5  
547 (2013).
- 548 23. Agnihotri, S. *et al.* A GATA4-regulated tumor suppressor network represses formation of  
549 malignant human astrocytomas. *J Exp Med* **208**, 689-702 (2011).
- 550 24. Hellebrekers, D.M. *et al.* GATA4 and GATA5 are potential tumor suppressors and biomarkers  
551 in colorectal cancer. *Clin Cancer Res* **15**, 3990-7 (2009).
- 552 25. Tsang, A.P. *et al.* FOG, a multitype zinc finger protein, acts as a cofactor for transcription  
553 factor GATA-1 in erythroid and megakaryocytic differentiation. *Cell* **90**, 109-19 (1997).
- 554 26. Adzhubei, I., Jordan, D.M. & Sunyaev, S.R. Predicting functional effect of human missense  
555 mutations using PolyPhen-2. *Curr Protoc Hum Genet* **Chapter 7**, Unit7 20 (2013).
- 556 27. Ketola, I. *et al.* Developmental expression and spermatogenic stage specificity of  
557 transcription factors GATA-1 and GATA-4 and their cofactors FOG-1 and FOG-2 in the mouse  
558 testis. *Eur J Endocrinol* **147**, 397-406 (2002).
- 559 28. Zheng, R. & Blobel, G.A. GATA Transcription Factors and Cancer. *Genes Cancer* **1**, 1178-88  
560 (2010).
- 561 29. Kurimoto, K., Yamaji, M., Seki, Y. & Saitou, M. Specification of the germ cell lineage in mice: a  
562 process orchestrated by the PR-domain proteins, Blimp1 and Prdm14. *Cell Cycle* **7**, 3514-8  
563 (2008).
- 564 30. Ohinata, Y. *et al.* A signaling principle for the specification of the germ cell lineage in mice.  
565 *Cell* **137**, 571-84 (2009).
- 566 31. Yamaji, M. *et al.* Critical function of Prdm14 for the establishment of the germ cell lineage in  
567 mice. *Nat Genet* **40**, 1016-22 (2008).
- 568 32. Smith, C.A., McClive, P.J., Western, P.S., Reed, K.J. & Sinclair, A.H. Conservation of a sex-  
569 determining gene. *Nature* **402**, 601-2 (1999).
- 570 33. Rao, S. *et al.* Differential roles of Sall4 isoforms in embryonic stem cell pluripotency. *Mol Cell*  
571 *Biol* **30**, 5364-80 (2010).
- 572 34. Greenbaum, M.P. *et al.* TEX14 is essential for intercellular bridges and fertility in male mice.  
573 *Proc Natl Acad Sci U S A* **103**, 4982-7 (2006).
- 574 35. Mondal, G., Ohashi, A., Yang, L., Rowley, M. & Couch, F.J. Tex14, a Plk1-regulated protein, is  
575 required for kinetochore-microtubule attachment and regulation of the spindle assembly  
576 checkpoint. *Mol Cell* **45**, 680-95 (2012).
- 577 36. Jinks, R.N. *et al.* Recessive nephrocerebellar syndrome on the Galloway-Mowat syndrome  
578 spectrum is caused by homozygous protein-truncating mutations of WDR73. *Brain* **138**,  
579 2173-90 (2015).
- 580 37. Colin, E. *et al.* Loss-of-function mutations in WDR73 are responsible for microcephaly and  
581 steroid-resistant nephrotic syndrome: Galloway-Mowat syndrome. *Am J Hum Genet* **95**, 637-  
582 48 (2014).
- 583 38. Petrovic, A. *et al.* The MIS12 complex is a protein interaction hub for outer kinetochore  
584 assembly. *J Cell Biol* **190**, 835-52 (2010).
- 585 39. Rao, C.V., Yamada, H.Y., Yao, Y. & Dai, W. Enhanced genomic instabilities caused by  
586 deregulated microtubule dynamics and chromosome segregation: a perspective from  
587 genetic studies in mice. *Carcinogenesis* **30**, 1469-74 (2009).
- 588 40. Barisic, M. *et al.* Mitosis. Microtubule detyrosination guides chromosomes during mitosis.  
589 *Science* **348**, 799-803 (2015).
- 590 41. Ma, W. & Viveiros, M.M. Depletion of pericentrin in mouse oocytes disrupts microtubule  
591 organizing center function and meiotic spindle organization. *Mol Reprod Dev* **81**, 1019-29  
592 (2014).



- 593 42. Litchfield, K. *et al.* Whole-exome sequencing reveals the mutational spectrum of testicular  
594 germ cell tumours. *Nat Commun* **6**, 5973 (2015).
- 595 43. Zeron-Medina, J. *et al.* A polymorphic p53 response element in KIT ligand influences cancer  
596 risk and has undergone natural selection. *Cell* **155**, 410-22 (2013).
- 597 44. De Miguel, M.P., Cheng, L., Holland, E.C., Federspiel, M.J. & Donovan, P.J. Dissection of the c-  
598 Kit signaling pathway in mouse primordial germ cells by retroviral-mediated gene transfer.  
599 *Proc Natl Acad Sci U S A* **99**, 10458-63 (2002).
- 600 45. Yu, M. *et al.* The scaffolding adapter Gab2, via Shp-2, regulates kit-evoked mast cell  
601 proliferation by activating the Rac/JNK pathway. *J Biol Chem* **281**, 28615-26 (2006).
- 602 46. Penegar, S. *et al.* National study of colorectal cancer genetics. *Br J Cancer* **97**, 1305-9 (2007).
- 603 47. Eisen, T., Matakidou, A., Houlston, R. & Consortium, G. Identification of low penetrance  
604 alleles for lung cancer: the GENetic Lung CANcer Predisposition Study (GELCAPS). *BMC*  
605 *Cancer* **8**, 244 (2008).
- 606 48. Delaneau, O., Marchini, J. & Zagury, J.F. A linear complexity phasing method for thousands  
607 of genomes. *Nat Methods* **9**, 179-81 (2012).
- 608 49. Howie, B., Fuchsberger, C., Stephens, M., Marchini, J. & Abecasis, G.R. Fast and accurate  
609 genotype imputation in genome-wide association studies through pre-phasing. *Nat Genet*  
610 **44**, 955-9 (2012).
- 611 50. Marchini, J. & Howie, B. Genotype imputation for genome-wide association studies. *Nat Rev*  
612 *Genet* **11**, 499-511 (2010).
- 613 51. Cuppen, E. Genotyping by Allele-Specific Amplification (KASPar). *CSH Protoc* **2007**, pdb  
614 prot4841 (2007).
- 615 52. Marchini, J., Howie, B., Myers, S., McVean, G. & Donnelly, P. A new multipoint method for  
616 genome-wide association studies by imputation of genotypes. *Nat Genet* **39**, 906-13 (2007).
- 617 53. Clayton, D.G. *et al.* Population structure, differential bias and genomic control in a large-  
618 scale, case-control association study. *Nat Genet* **37**, 1243-6 (2005).
- 619 54. Litchfield, K. *et al.* Multi-stage genome wide association study identifies new susceptibility  
620 locus for testicular germ cell tumour on chromosome 3q25. *Hum Mol Genet* (2014).
- 621 55. Liu, J.Z. *et al.* Meta-analysis and imputation refines the association of 15q25 with smoking  
622 quantity. *Nat Genet* **42**, 436-40 (2010).
- 623 56. Higgins, J.P. & Thompson, S.G. Quantifying heterogeneity in a meta-analysis. *Stat Med* **21**,  
624 1539-58 (2002).
- 625 57. Scales, M., Jager, R., Migliorini, G., Houlston, R.S. & Henrion, M.Y. visPIG--a web tool for  
626 producing multi-region, multi-track, multi-scale plots of genetic data. *PLoS One* **9**, e107497  
627 (2014).
- 628 58. Pharoah, P.D.P. *et al.* Polygenic susceptibility to breast cancer and implications for  
629 prevention. *Nature Genetics* **31**, 33-36 (2002).
- 630 59. Cancer Research UK 2014, Testicular Cancer Life Time Risk, Cancer Research UK.
- 631 60. Cowper-Salari, R. *et al.* Breast cancer risk-associated SNPs modulate the affinity of  
632 chromatin for FOXA1 and alter gene expression. *Nat Genet* **44**, 1191-8 (2012).
- 633 61. Rao, S.S. *et al.* A 3D map of the human genome at kilobase resolution reveals principles of  
634 chromatin looping. *Cell* **159**, 1665-80 (2014).
- 635 62. Mifsud, B. *et al.* Mapping long-range promoter contacts in human cells with high-resolution  
636 capture Hi-C. *Nat Genet* **47**, 598-606 (2015).
- 637 63. Wingett, S. *et al.* HiCUP: pipeline for mapping and processing Hi-C data. *F1000Res* **4**, 1310  
638 (2015).
- 639 64. Jonathan Cairns, P.F.-P., Steven W. Wingett, Csilla Várnai, Andrew Dimond, Vincent Plagnol,  
640 Daniel Zerbino, Stefan Schoenfelder, Biola-Maria Javierre, Cameron Osborne, Peter Fraser,

641 Mikhail Spivakov. CHiCAGO: Robust Detection of DNA Looping Interactions in Capture Hi-C  
642 data. *BioRxiv* (2016).

643 65. Untergasser, A. *et al.* Primer3--new capabilities and interfaces. *Nucleic Acids Res* **40**, e115  
644 (2012).

645 66. Schneider, C.A., Rasband, W.S. & Eliceiri, K.W. NIH Image to ImageJ: 25 years of image  
646 analysis. *Nat Methods* **9**, 671-5 (2012).

647 67. Ernst, J. & Kellis, M. ChromHMM: automating chromatin-state discovery and  
648 characterization. *Nat Methods* **9**, 215-6 (2012).

649 68. Hamosh, A., Scott, A.F., Amberger, J.S., Bocchini, C.A. & McKusick, V.A. Online Mendelian  
650 Inheritance in Man (OMIM), a knowledgebase of human genes and genetic disorders.  
651 *Nucleic Acids Res* **33**, D514-7 (2005).

652 69. Ward, L.D. & Kellis, M. HaploReg: a resource for exploring chromatin states, conservation,  
653 and regulatory motif alterations within sets of genetically linked variants. *Nucleic Acids Res*  
654 **40**, D930-4 (2012).

655 70. Kheradpour, P. & Kellis, M. Systematic discovery and characterization of regulatory motifs in  
656 ENCODE TF binding experiments. *Nucleic Acids Res* **42**, 2976-87 (2014).

657 71. Zerbino, D.R., Wilder, S.P., Johnson, N., Juettemann, T. & Flicek, P.R. The ensembl regulatory  
658 build. *Genome Biol* **16**, 56 (2015).

659

660

## GWAS & replication

Oncoarray  
3,206 cases  
7,422 controls

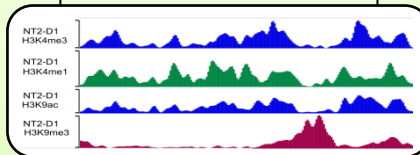
Published GWAS  
2,312 cases  
11,633 controls

Meta-GWAS discovery  
5,518 cases / 19,055 controls

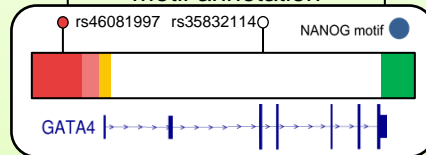
Replication genotyping  
1,801 cases / 4,027 controls

## Functional annotation

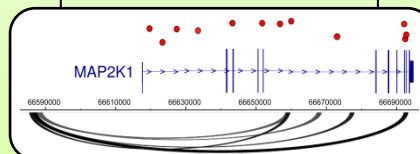
ChIP-seq  
chromatin profiling



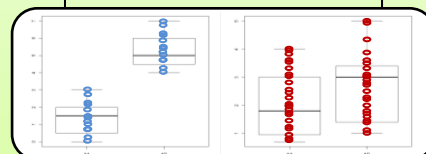
Promoter/coding  
variant & TF binding  
motif annotation



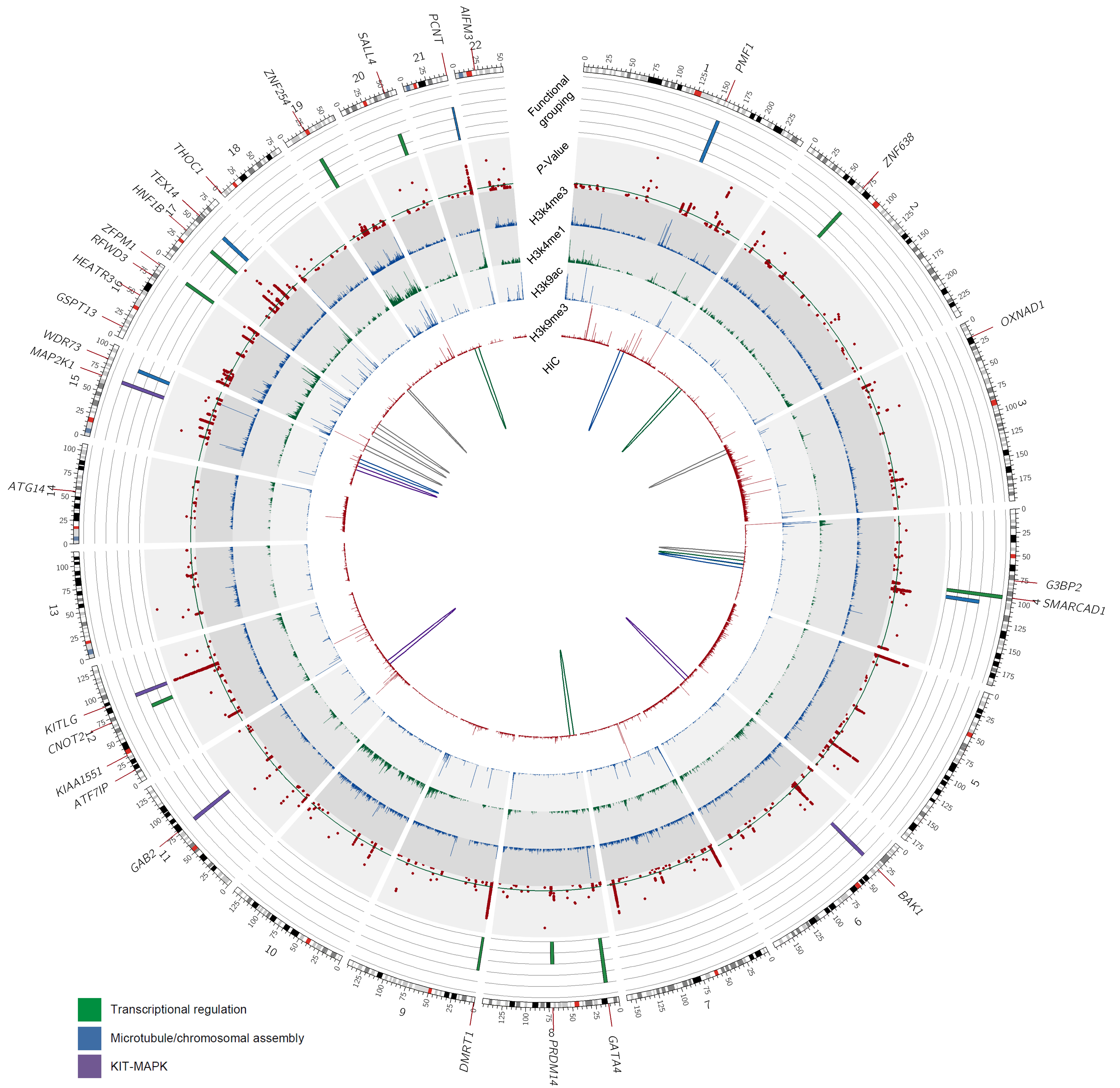
HiC promoter capture



eQTL analysis







- Transcriptional regulation
- Microtubule/chromosomal assembly
- KIT-MAPK



Figure 3A.

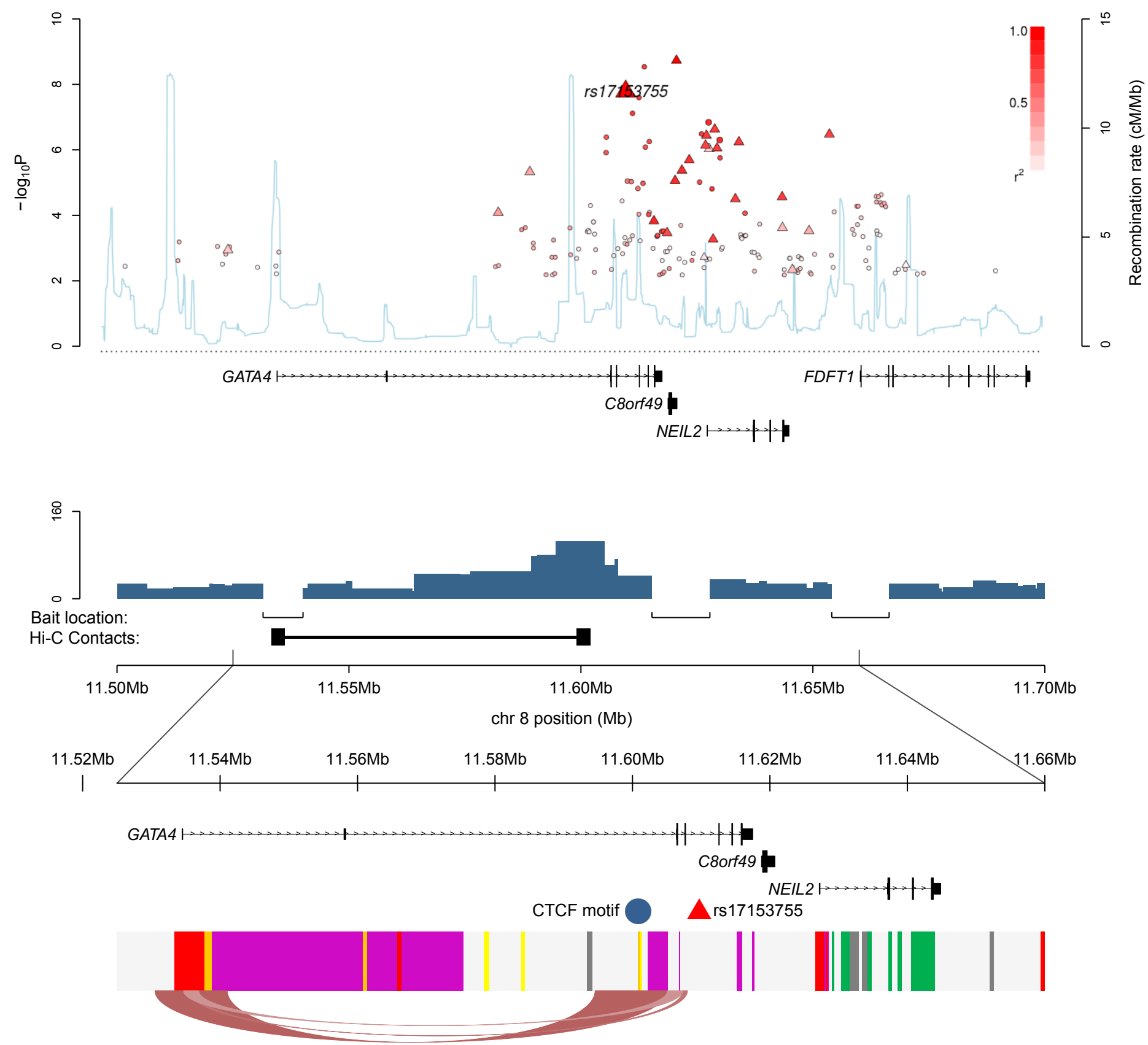


Figure 3B.

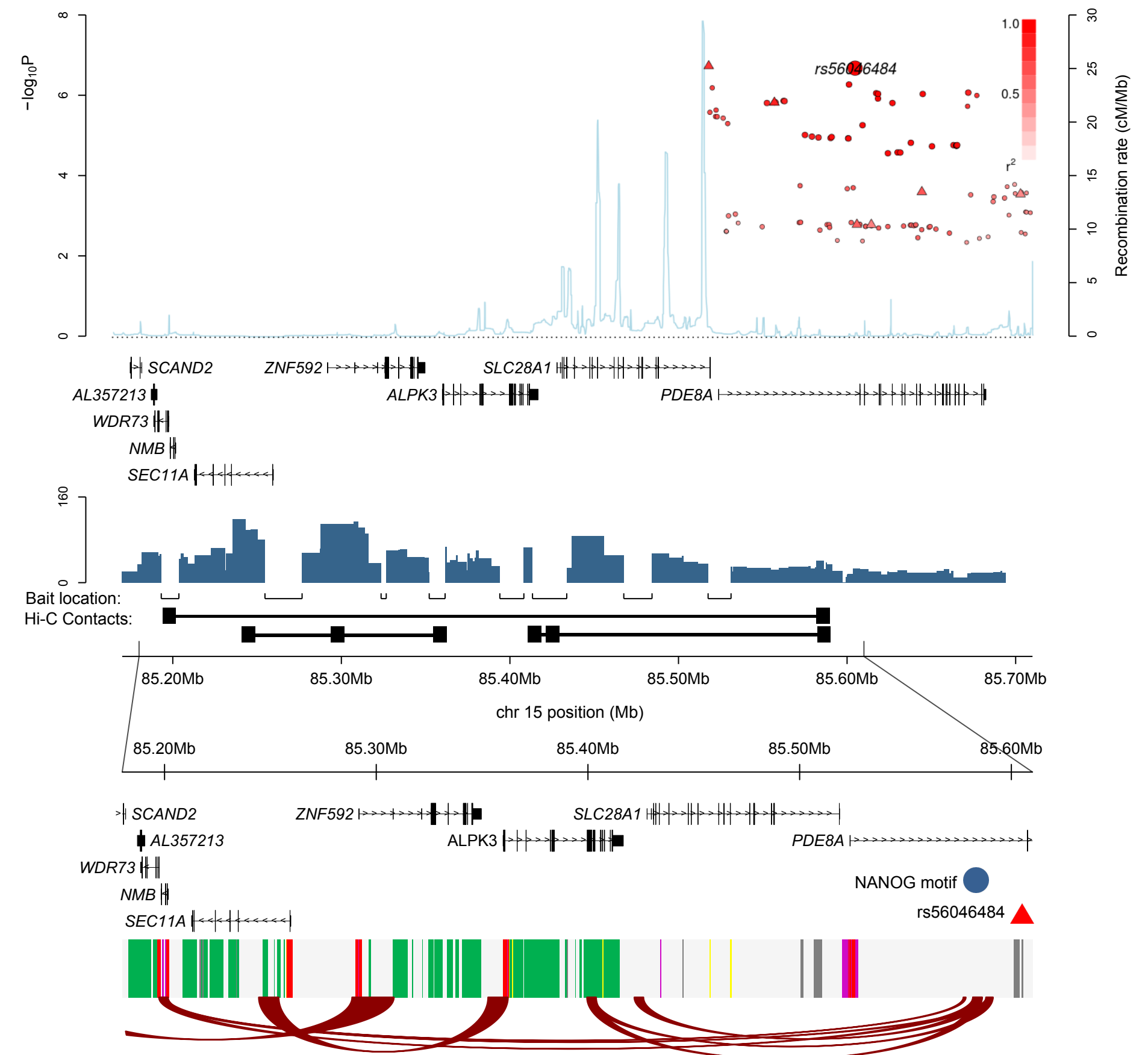


Figure 3C.

